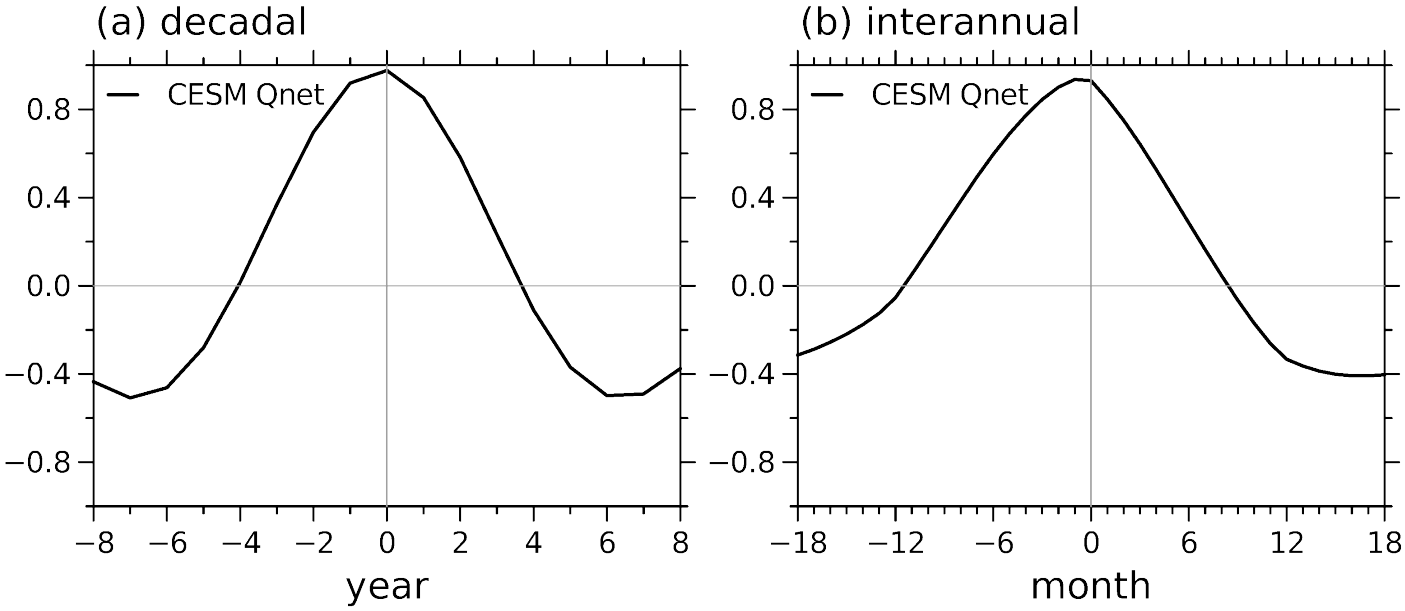

Fig. S1: As in Figs. 2e,j, respectively, but for global net surface heat flux (Q_{net}; positive values for downward flux).

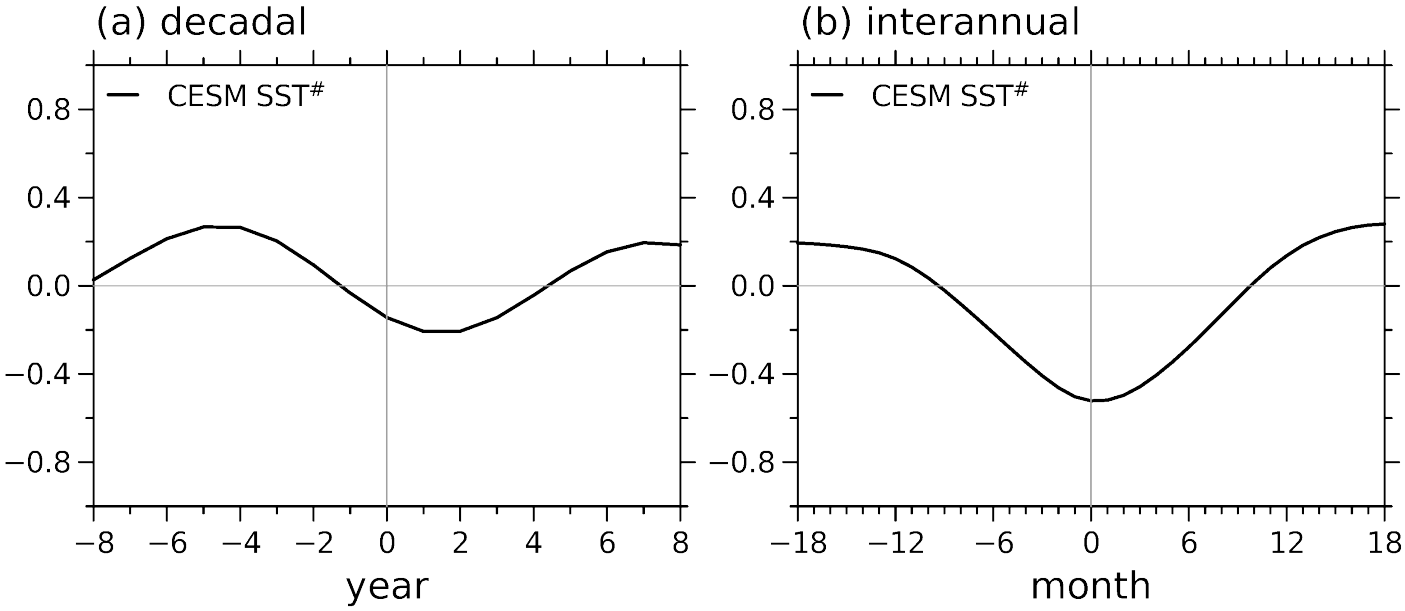

Fig. S2: As in Figs. 2e,j, respectively, but for the SST$^{\#}$ index. Following Fueglistaler (2019), the SST$^{\#}$ index is defined as the temperature of the warmest 30% minus the tropical (30ºS-30ºN) average SST.

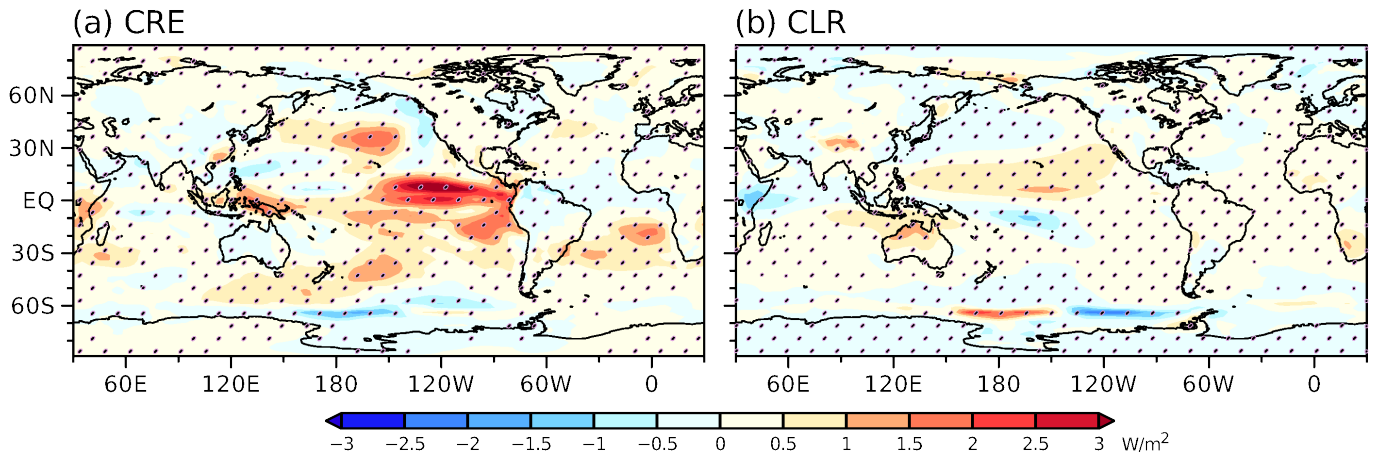

Fig. S3: Regression maps of TOA CRE (a) and clear-sky flux (b) anomalies onto CESM interannual GMTOA at lag 0. Stippling signifies the 90% confidence. Units is W m^{-2}.

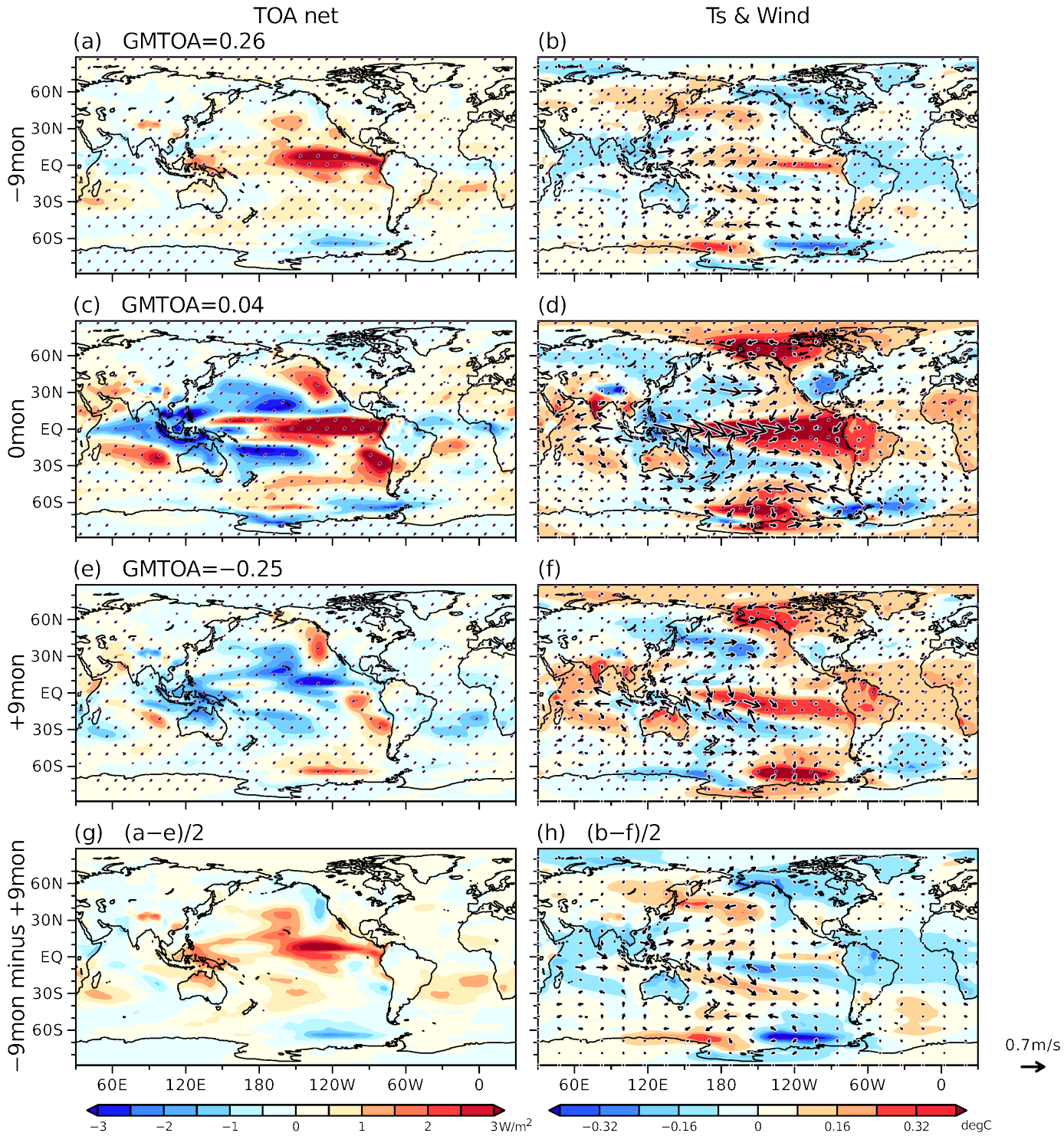

Fig. S4: ENSO-related anomalies. Lagged regression maps of (a,c,e) TOA radiation (W m^{-2}; GMTOA are shown in the title), (b,d,f) surface temperature (shading; ºC) and wind (arrows; m s^{-1}; only points with the 90% confidence are drawn) onto interannual Nino3.4 SST anomalies at lags (a,b) –9, (c,d) 0, and (e,f) +9 months. Corresponding GMTOA anomalies are shown. Stippling indicates the 90% confidence. (g,h) the bulk ENSO-related anomalies as the half of the difference between lag –9 and +9 months, following Ceppi and Fueglistaler (2021). Results are insensitive among lags ±8,9,10 months near the peak correlation with GMTOA.

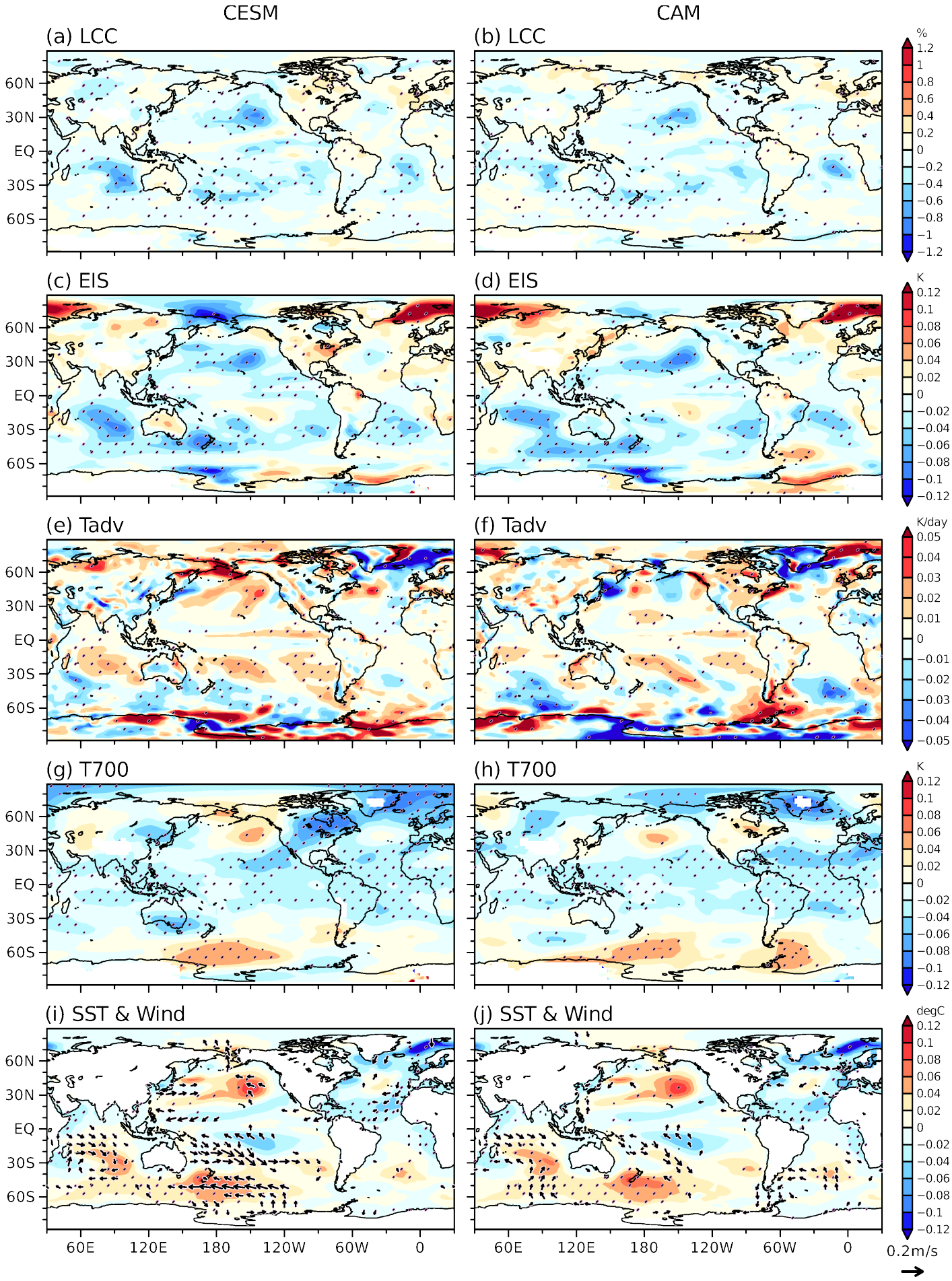

Fig. S5: As in Fig. 7, but for lag 0.

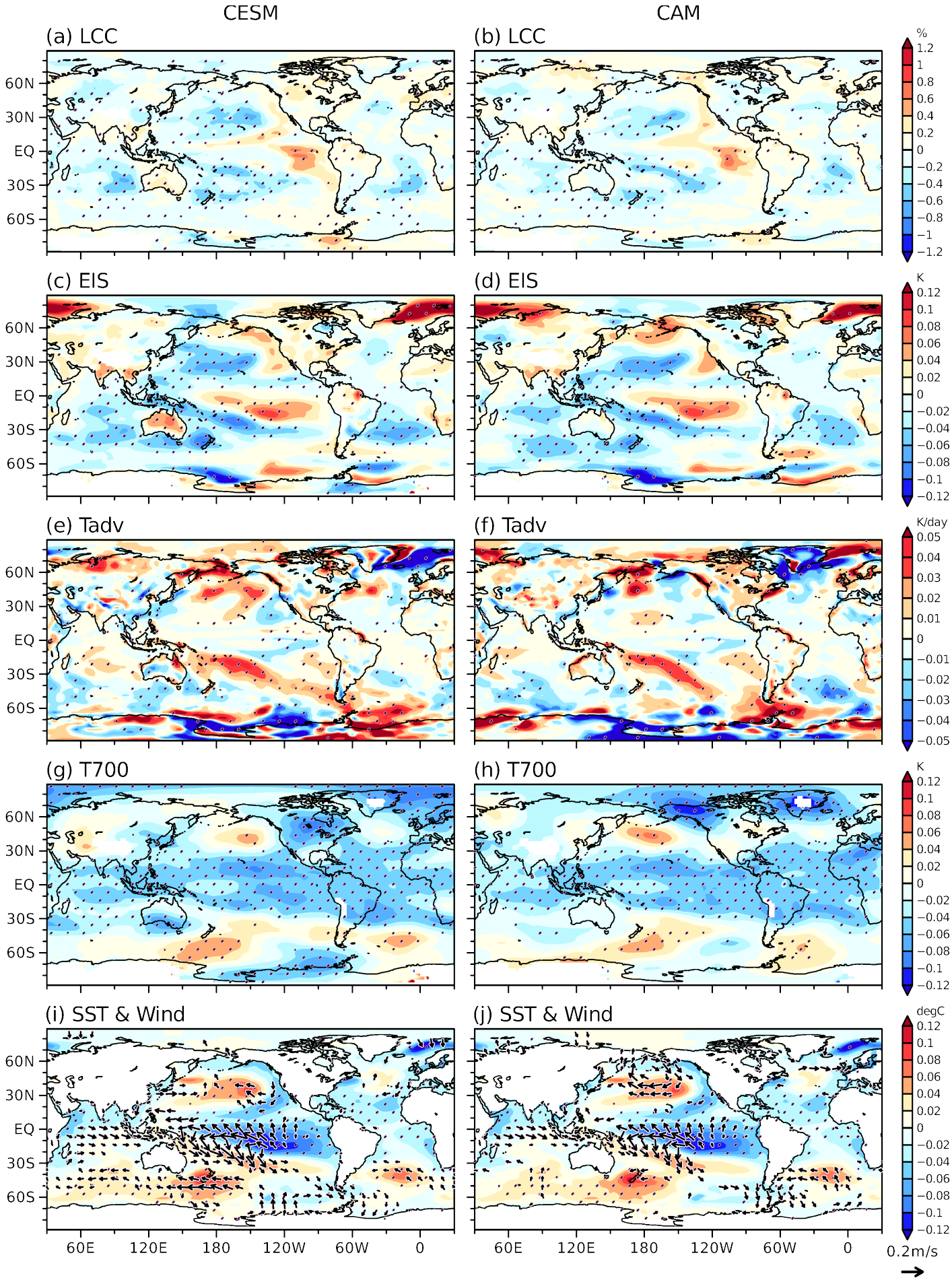

Fig. S6: As in Fig. 7, but for lag –1 year.

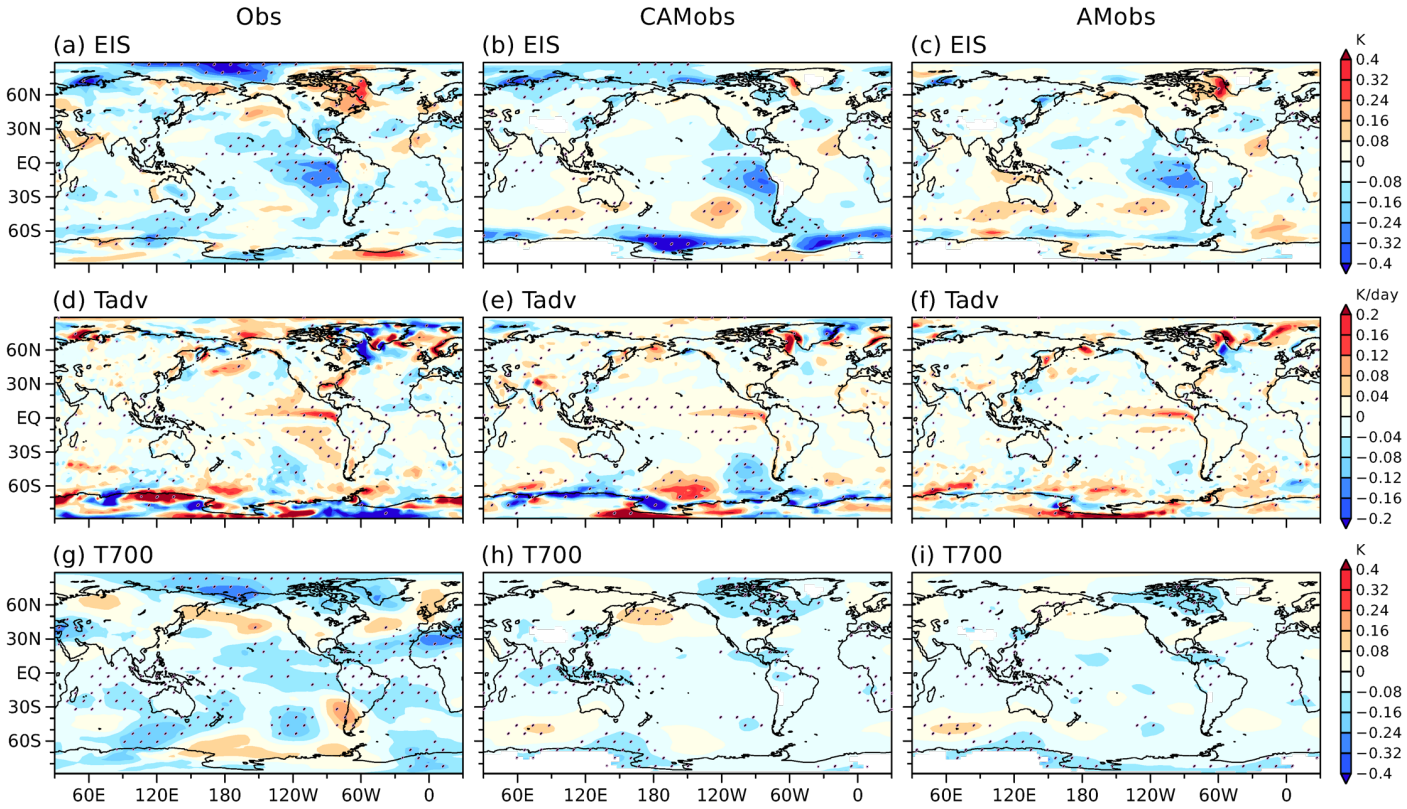

Fig. S7: As in Fig. 9, but (a,b,c) EIS (K), (d,e,f) surface temperature advection (K day^{-1}), and (g,h,i) 700-hPa temperature (K).